Published OnlineFirst June 9, 2015; DOI: 10.1158/1078-0432.CCR-15-0423

Biology of Human Tumors

Clinical Cancer Research

Deep Sequencing Reveals Occurrence of Subclonal *ALK* Mutations in Neuroblastoma at Diagnosis

Angela Bellini[1,2], Virginie Bernard[3], Quentin Leroy[3], Thomas Rio Frio[3], Gaelle Pierron[4], Valérie Combaret[5], Eve Lapouble[4], Nathalie Clement[1,6], Herve Rubie[7], Estelle Thebaud[8], Pascal Chastagner[9], Anne Sophie Defachelles[10], Christophe Bergeron[11], Nimrod Buchbinder[12], Sophie Taque[13], Anne Auvrignon[14], Dominique Valteau-Couanet[15], Jean Michon[6], Isabelle Janoueix-Lerosey[2], Olivier Delattre[2,4], and Gudrun Schleiermacher[1,2,6]

Abstract

Purpose: In neuroblastoma, activating *ALK* receptor tyrosine kinase point mutations play a major role in oncogenesis. We explored the potential occurrence of *ALK* mutations at a subclonal level using targeted deep sequencing.

Experimental Design: In a clinically representative series of 276 diagnostic neuroblastoma samples, exons 23 and 25 of the *ALK* gene, containing the F1174 and R1275 mutation hotspots, respectively, were resequenced with an extremely high depth of coverage.

Results: At the F1174 hotspot (exon 23), mutations were observed in 15 of 277 samples (range of fraction of mutated allele per sample: 0.562%–40.409%). At the R1275 hotspot (exon 25), *ALK* mutations were detected in 12 of 276 samples (range of fraction of mutated allele: 0.811%–73.001%). Altogether, subclonal events with a mutated allele fraction below 20% were observed in 15/27 *ALK*-mutated samples. The presence of an *ALK* mutation was associated with poorer 5-year overall survival (OS: 75% vs. 57%, $P = 0.0212$ log-rank test), with a strong correlation between *F1174 ALK* mutations and *MYCN* amplification being observed.

Conclusions: In this series, deep sequencing allows the detection of F1174 and R1275 *ALK* mutational events at diagnosis in 10% of cases, with subclonal events in more than half of these, which would have gone undetected by Sanger sequencing. These findings are of clinical importance given the potential role of *ALK* mutations in clonal evolution and relapse. These findings also demonstrate the importance of deep sequencing techniques for the identification of patients especially when considering targeted therapy. *Clin Cancer Res; 21(21); 4913–21. ©2015 AACR.*

See related commentary by George, p. 4747

Introduction

Intratumor heterogeneity has been shown to occur in the majority of human malignancies, including chromosomal alterations or gene mutations, and has been shown to play a role in clonal evolution (1–6).

With fractions of mutated alleles evolving over time, the study of the exact mutated allele fractions, of their subclonal distribution and possible role in clonal evolution gains more importance (7–9).

In neuroblastoma, the most frequent extracranial solid cancer of early childhood, efforts to develop improved therapies must also take into account its molecular heterogeneity. Genetic alterations in neuroblastoma at diagnosis mainly concern copy number alterations, with MYCN amplification in 20% to 25% of cases, and segmental copy number alterations involving more extensive chromosome regions (10–14). Genome sequencing studies of neuroblastoma at diagnosis have revealed a low mutation rate involving only few recurrently altered genes mainly involved in chromatin-remodeling or neuritogenesis (15–17).

Activating anaplastic lymphoma kinase (*ALK*) mutations have been shown to occur in both familial and sporadic cases of

[1]Equipe SiRIC RTOP Recherche Translationelle en Oncologie Pédiatrique, Institut Curie, Paris, France. [2]INSERM U830, Laboratoire de Génétique et Biologie des Cancers, Institut Curie, Paris, France. [3]Plateforme de Séquençage ICGex, Institut Curie, Paris, France. [4]Unité de Génétique Somatique, Institut Curie, Paris, France. [5]Laboratoire de Recherche Translationnelle, Centre Léon-Bérard, Lyon, France. [6]Département de Pédiatrie, Institut Curie, Paris, France. [7]Unite d'Hemato-Oncologie, Hôpital des Enfants, Toulouse, France. [8]Service d'Hémato-Oncologie Pédiatrique, CHU Nantes, Nantes, France. [9]Service d'Immuno-Hémato-Oncologie, Hôpital d'Enfants, Nancy, France. [10]Service d'Oncologie Pédiatrique, Centre Oscar Lambret, Lille, France. [11]Institut d'Hematologie et d'Oncologie Pédiatrique, Centre Léon Bérard, Lyon, France. [12]Service d'Immuno-Hémato-Oncologie Pédiatrique, Hôpital Charles Nicolle, Rouen, France. [13]Service d'Hématologie et de Cancérologie, CHU Hôpital Sud, Rennes, France. [14]Service d'Hématologie et d'Oncologie Pédiatrique, Hôpital d'Enfants Armand-Trousseau, Paris, France. [15]Departement de Pédiatrie, Institut Gustave Roussy, Villejuif, France.

Note: Supplementary data for this article are available at Clinical Cancer Research Online (http://clincancerres.aacrjournals.org/).

Corresponding Author: Gudrun Schleiermacher, Department of Pediatric Oncology, Institut Curie, 26 rue d'Ulm, 75248 Paris Cedex 05, France. Phone: 033-1-44-32-45-50; Fax: 33-1-53-10-40-05; E-mail: gudrun.schleiermacher@curie.fr

doi: 10.1158/1078-0432.CCR-15-0423

Published OnlineFirst June 9, 2015; DOI: 10.1158/1078-0432.CCR-15-0423

Translational Relevance

In neuroblastoma, conventional sequencing techniques allowed the detection of *ALK* gene mutations in familiar and sporadic cases. In this study, we search for *ALK* mutations in neuroblastoma samples at diagnosis by using high sensitivity next-generation sequencing (NGS) methods. *ALK* mutations were observed at diagnosis in 10% of cases, with *ALK* mutational events showing a fraction of mutated alleles lower than 20%, at the subclonal level, in more than half of these samples. This study provides important evidence for the usefulness of deep-sequencing NGS methods to reveal the presence of very low mutated allele fractions undetectable with conventional Sanger sequencing, and demonstrates the importance of deep-sequencing techniques in particular in the context of potential identification of predictive biomarkers when considering target therapy.

neuroblastoma, with somatically acquired *ALK* mutations observed in 6% to 12% of sporadic neuroblastomas (15, 16, 18–21). The most frequent substitutions, observed in approximately 85% of mutant *ALK* in neuroblastoma, are localized within the kinase domain of *ALK* at the F1174 (mutated to L, S, I, C, or V) and R1275 (mutated to Q or L) hotspots (12, 21). In neuroblastoma, *ALK* can also be activated by genomic amplification (approximately 1%–2% of neuroblastomas) or more rarely following structural rearrangements (22).

Activating *ALK* mutations are thought to play a role in neuroblastoma oncogenesis based on *in vitro* and *in vivo* observations, in some instances through collaboration with MYCN (23–25). Thus, *ALK* might represent a *bone fide* target in neuroblastoma therapy. We have recently used deep sequencing to search for *ALK* mutations in neuroblastoma relapse samples (26). Furthermore, in a recent study, the feasibility of a new method of *ALK* mutations detection in circulating tumor DNA (ctDNA) using droplet digital PCR (ddPCR) has been described. This method showed the presence of the F1174L and R1275Q *ALK* mutations in circulating DNA from 21% of neuroblastoma patients at diagnosis (27). Altogether, these studies highlight the importance of next-generation deep sequencing techniques when determining the genetic status of this predictive biomarker.

In order to detect *ALK* mutations with a high sensitivity and to determine the frequency of subclonal events in neuroblastoma, we have now analyzed a series of 276 diagnostic neuroblastoma samples using targeted deep sequencing.

Materials and Methods

Patients and samples

Patients with neuroblastoma for whom a tumor sample was addressed to the laboratory for diagnostic molecular analysis were included in this study to constitute a representative neuroblastoma patient cohort. For a total of 276 patients, 125 patients with stage IV disease (46%), 123 with localized disease (44%), 25 with stage 4s disease (9%), and 55 patients with MYCN amplification (20%) were included (Supplementary Table S1). Pathologic examination by hematoxylin and eosin (H&E) staining method documented at least 50% of tumor cells in all samples.

MYCN status and tumor genomic copy number profiles were determined as described previously, using an in-house 4k or a commercial 72k platform (Nimblegen; ref. 6).

Patients were treated in French centers according to the relevant national or international protocols. Written informed consent was obtained from parents according to national law and Ethics approval of protocols was obtained according to national guidelines. This study was authorized by the ethics committees "Comité de Protection des Personnes Sud-Est IV," references L07–95/L12–171, and "Comité de Protection des Personnes Ile de France," reference 0811728.

Twenty-four germline genomic DNAs from CEPH (Centre d'Etude du Polymorphisme Humain) from healthy donors served as controls.

Library preparation

For sequencing library construction, 50 ng of genomic DNA from each sample were used to amplify the *ALK* regions of interest (exon 23:chr2:29443647–29443776; exon 25: chr2:29432603–29432704). The regions containing *ALK* hotspots F1174 (exon 23) and R1275 (exon 25) were amplified in a two-step PCR procedure using the Phusion Hot Start II high fidelity DNA polymerase (Thermo Scientific). During the first PCR round, region-specific primers with adapter overhang on both forward and reverse primers (Supplementary Table S2) were used for a total of 10 cycles. The second PCR round, for a total of 30 cycles, attached Illumina single direction primers at the ends of amplicons. The adapter sequences and the unique barcodes contained in the Illumina primers were added at the 3′ and 5′ ends, respectively [Access Array Barcode Library for Illumina Sequencers 384 (Single direction) P/N 100-4876]. Following clean-up using the vacuum ultrafiltration kit (Macherey Nagel), control of size range using LabChip devices (Caliper, PerkinElmer) and Qubit quantification, PCR products of all samples were then pooled together in an equimolar solution: the cases to be studied, the germline controls, and negative controls. The final pooled library was then loaded on the HiSeq2500 flow cell.

The library was sequenced using the paired-end procedure on the Illumina Hiseq2500 according to the manufacturer. Sample barcoding enabled 384 individual samples to be sequenced on each lane, aiming for a depth of coverage of at least 16,000X for the amplicons in every sample (Fig. 1).

Bioinformatics detection of variations

Once paired-end reads merged and adaptors trimmed by SeqPrep with default parameters, merged reads were aligned via BWA allowing up to one difference in the 22-base-long seeds and reporting only unique alignments (26).

Variant calling software was not used, since we aimed to predict also variations at low frequencies. Such variants require a custom approach using DepthOfCoverage functions of the Genome Analysis Toolkit (GATK) v2.13.2 and additional statistical analysis (28).

In order to focus on high-quality data, only reads with a mapping quality of >20 and a base quality of >10 were considered for the determination of the depth of coverage. First, in order to analyze the noise and to determine the background level of variability over the studied regions, the entire amplicons chr2:29443647–29443776 and chr2:29432603–29432704 (Human Genome Browser, http://genome.ucsc.edu/; hg19) were analyzed in 24 germline control samples.

Published OnlineFirst June 9, 2015; DOI: 10.1158/1078-0432.CCR-15-0423

Next, in order to highlight variants in the neuroblastoma samples, for each sample the frequencies of each base at each position were compared with those observed in the germline controls. Statistical analyses were performed with the R statistical software (http://www.R-project.org). Fisher exact two-side tests with a Bonferroni correction were performed to compare percentages of base frequencies (allele fractions) between the datasets, that is, for a given base between a case and the controls. It takes into account for each coordinate and each base the impact of its environment since controls were sequenced together with cases for comparison. In complement, in order to limit false-positive predictions of variants, we kept as *P* value threshold the lowest one within intronic regions of the amplicons once polymorphisms filtered, since no causal variants were expected in those regions (exon 23: 1.1E−154 and exon 25: 6.1E−193, respectively). Finally, significant variations were filtered-in once (i) a significant increase in the percentage of variant base and (ii) a significant decrease in the percentage of its reference base following our *P* values criteria were observed.

The experiments were performed twice in an independent manner with the same approach. Only results predicted twice were considered.

Statistical analysis

Correlation analyses using χ^2 test and survival analysis using multivariate logistic regression analysis were done with MedCalc (Medical Calculator) software (version 13.3.0.0). Progression-free survival (PFS) and overall survival (OS) were estimated using the Kaplan–Meier method, and comparisons were made using log-rank tests.

Results

In order to determine the frequency of *ALK* mutations with a higher sensitivity than conventional Sanger sequencing, we sequenced the *ALK* F1174 and R1275 hotspots in a series of 276 neuroblastoma samples in a two-step PCR procedure using HiSeq technology with a very high depth of coverage (Supplementary Table S1).

Background variability

In a first step, the sensitivity of the technique across a series of 24 germline controls was determined. The mean overall depth of coverage for the germline controls was 33,000X (range, 25069–56620) for the exon23 and 41,000X (range, 25062–56639) for the exon25 amplified region, respectively (Fig. 1). At this deep coverage, within targeted regions, the mean overall background variability, or noise, was 0.014% ± 0.031% in the germline controls (Supplementary Fig. S1).

To determine the expected sensitivity, we then calculated for each position the number of variation-supporting reads that would result in a statistically significant difference from the background noise. Bonferroni correction was applied, as multiple tests were performed for each base at each position. Considering a mean coverage of 33,000X, a variation supported by 688 reads or more, or observed with a frequency higher than 0.21%, would result in a statistically significant difference from the controls (two-sided Fisher exact test; details in Materials and Methods).

In the studied neuroblastoma samples, the depth of coverage and the overall background variability was not different from that observed in the germline controls. Furthermore, except a variant reported in dbSNP and in the 1000Genomes project (PMID:11125122) as a polymorphism (rs3738868) observed in more than 1% of the population (chr2:29432625, G>T), no variants outside the studied hotspots were observed in the targeted regions.

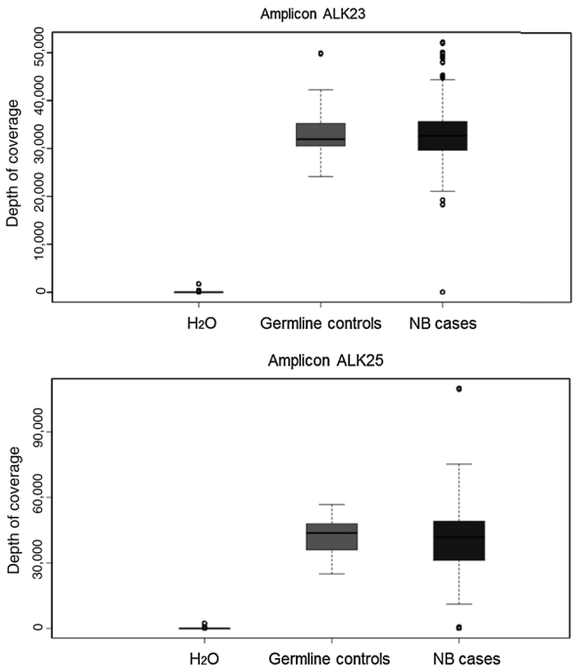

Figure 1.
Boxplots showing the overall depth of coverage achieved by Hiseq2500 Illumina deep-sequencing of *ALK* targeted regions. The boxplot depicts the distribution of mean depth of coverage of H_2O negative controls, germline controls, and neuroblastoma samples over the exon 23 (A) and exon 25 (B) targeted regions. This representation shows the very high depth of coverage achieved for neuroblastoma samples (at least 16000X). The mean overall coverage in the germline controls is 33000X and 41000X for F1174 and R1275 hotspots, respectively. H_2O negative controls show an extremely low depth of coverage (mean = 58X for F1174 and 85X for R1275).

Mutations detected in exons 23 and 25

In a next step, the mutational status of the *ALK* gene within exons 23 and 25 at the hotspots F1174 and R1275 was analyzed. At positions chr2:29443695–29443697 (F1174 hotspot), *ALK* mutations were observed in 15 cases: 13 cases harbored a mutation leading to the amino acid change F1174L; F1174C and F1174V were each detected in one case, with a range of fractions of the mutated allele of 0.562% to 40.409% (Table 1, panel A). At position chr2:29432664 (R1275 hotspot), *ALK* mutations were detected in 12 cases: 11 samples showed the R1275Q mutation and one case showed the R1275L mutation, with a range of mutated allele fractions from 0.811% to 73.001% (Table 1, panel B).

Altogether, deep sequencing revealed the presence of *ALK* mutations at the two hotspots F1174 and R1275 in 27/276 (9.8%) samples (Fig. 2; Table 2), with a wide range of mutated allele fractions (range: 0.562%–73.001%), even when corrected for tumor cell content and chr2p copy number status (Table 2 and Supplementary Table S1).

Published OnlineFirst June 9, 2015; DOI: 10.1158/1078-0432.CCR-15-0423

Table 1. Base frequencies (mutated allele fractions) at the F1174 (A) and R1275 (B) hotspots in samples analyzed by targeted deep sequencing

A

Chr position/ patient no.	Number of reads	T		G		C		A		Codon change	AA change
		%	*P*	%	*P*	%	*P*	%	*P*		
chr2:29443695											
NB0012T	31,826	0.006	NS	0.000	NS	92.336	<1E−200	**7.657**	<1E−200	TTC>TT**A**	F1174**L**
NB0014T	34,146	0.015	NS	0.003	NS	99.239	2.20E−227	**0.744**	7.55E−266	TTC>TT**A**	F1174**L**
NB0183T	91,783	0.007	NS	0.004	NS	99.202	<1E−200	**0.787**	<1E−200	TTC>TT**A**	F1174**L**
NB0186T	34,516	0.012	NS	0.003	NS	89.289	<1E−200	**10.691**	<1E−200	TTC>TT**A**	F1174**L**
NB0194T	87,354	0.003	NS	0.002	NS	95.075	<1E−200	**4.914**	<1E−200	TTC>TT**A**	F1174**L**
NB0230T	31,837	0.003	NS	0.000	NS	99.435	3.76E−143	**0.562**	5.21E−178	TTC>TT**A**	F1174**L**
NB0231T	29,605	0.003	NS	0.000	NS	97.247	<1E−200	**2.75**	<1E−200	TTC>TT**A**	F1174**L**
NB0284T	34,364	0.017	NS	**0.917**	<1E-200	99.057	1.83E−301	0.009	NS	TTC>TT**G**	F1174**L**
NB0366T	38,842	0.013	NS	0.003	NS	77.957	<1E−200	**22.025**	<1E−200	TTC>TT**A**	F1174**L**
NB0824T	38,744	0.003	NS	0.008	NS	76.19	<1E−200	**23.795**	<1E−200	TTC>TT**A**	F1174**L**
NB1244T	32,971	0.012	NS	0.003	NS	86.521	<1E−200	**13.46**	<1E−200	TTC>TT**A**	F1174**L**
Controls (ALL)	796,066	0.009	NS	0.003	NS	99.976	NS	0.011	NS	—	—
chr2:29443696											
NB0920T	31,033	59.585	<1E−200	**40.409**	<1E−200	0.006	NS	0.000	NS	TTC>T**G**C	F1174**C**
Controls (ALL)	796,952	99.987	NS	0.000	NS	0.009	NS	0.004	NS	—	—
chr2:29443697											
NB0535T	36,776	78.116	<1E−200	**21.772**	<1E−200	0.111	3.94E−20	0.000	NS	TTC>**G**TC	F1174**V**
NB0789T	29,509	76.963	<1E−200	0.000	NS	**23.037**	<1E−200	0.000	NS	TTC>**C**TC	F1174**L**
NB1253T	33,950	94.677	<1E−200	0.000	NS	**5.323**	<1E−200	0.000	NS	TTC>**C**TC	F1174**L**
Controls (ALL)	79,7051	99.987	NS	0.000	NS	0.01	NS	0.003	NS	—	—

B

Chr position/ patient no.	Number of reads	T		G		C		A		Codon change	AA change
		%	*P*	%	*P*	%	*P*	%	*P*		
chr2:29432664											
NB0085T	54,995	0.004	NS	38.267	<1E−200	0.004	NS	**61.722**	<1E−200	CGA>C**A**A	R1275**Q**
NB0211T	48,445	0.014	NS	71.335	<1E−200	0.004	NS	**28.647**	<1E−200	CGA>C**A**A	R1275**Q**
NB0222T	54,010	**49.206**	<1E−200	50.737	<1E−200	0.007	NS	0.046	NS	CGA>C**T**A	R1275**L**
NB0233T	41,581	0.019	NS	96.325	<1E−200	0.002	NS	**3.648**	<1E−200	CGA>C**A**A	R1275**Q**
NB0308T	31,473	0.000	NS	85.581	<1E−200	0.000	NS	**14.419**	<1E−200	CGA>C**A**A	R1275**Q**
NB0372T	18,256	0.011	NS	38.541	<1E−200	0.005	NS	**61.443**	<1E−200	CGA>C**A**A	R1275**Q**
NB0540T	30,453	0.013	NS	99.176	1.48E−189	0.000	NS	**0.811**	1.03E−222	CGA>C**A**A	R1275**Q**
NB0984T	16,681	0.006	NS	54.865	<1E−200	0.000	NS	**45.123**	<1E−200	CGA>C**A**A	R1275**Q**
NB1001T	35,339	0.025	NS	64.47	<1E−200	0.006	NS	**35.499**	<1E−200	CGA>C**A**A	R1275**Q**
NB1057T	30,841	0.003	NS	96.887	<1E−200	0.000	NS	**3.109**	<1E−200	CGA>C**A**A	R1275**Q**
NB1129T	27,138	0.000	NS	96.002	<1E−200	0.004	NS	**3.994**	<1E−200	CGA>C**A**A	R1275**Q**
NB1418T	48,236	0.012	NS	26.976	<1E−200	0.004	NS	**73.001**	<1E−200	CGA>C**A**A	R1275**Q**
Controls (ALL)	100,586,7	0.016	NS	99.956	NS	0.001	NS	0.027	NS	—	—

NOTE: The base corresponding to the reference genome (Human Genome Browser, http://genome.ucsc.edu/; hg19) is indicated at a given coordinate. For a sample to be analyzed, the total number of high-quality reads obtained by Hiseq deep sequencing is indicated, and the percentage of reads supporting each base (A, C, G, T) is shown. Values reported for controls are calculated from the total number of reads for germline controls at the given position. The mean base frequencies observed in the control set is also indicated. For each case, the *P* value refers to the comparison (two-sided Fisher exact test) of the base frequency observed in the studied sample to that observed in the controls. Statistically relevant differences are indicated in bold.

Abbreviations: AA, amino acid; NS, not statistically significant.

Indeed, in this study, contamination with normal cells should be considered. For this study, contamination of tumor samples by normal cells of up to 50% was tolerated, and thus it is expected that in these samples heterozygous mutations would be present in 25% of all analyzed DNA fragments in a diploid context when occurring in all tumor cells. Thus, we use the term "clonal" for a mutated allele fraction > 20%, which would most likely concern a majority of tumor cells, and the term "subclonal" for a mutated allele fraction < 20%, which would most likely concern a smaller tumor cell population. On the basis of this definition and on the deep-sequencing results, 12 *ALK* mutations observed with an allele fraction higher than 20% might be considered as clonal, whereas 15 *ALK* mutations detected with an allele fraction of lower than 20% might be considered as subclonal events.

All deep-sequencing results were validated in a second independent experiment. Concordance between the first and second experiments was documented by (i) concordance of mutated allele fractions in the neuroblastoma samples between the two separate experiments and by (ii) concordance of frequencies of the allele of the rs3738868 polymorphism (Supplementary Fig. S2). Only in two of 276 cases was a discordance observed between the first and the second experiment and these cases were excluded from the analysis, both detected at very low mutated allele fractions in one experiment but not the other. These results indicate a very low false discovery rate of 2/276 (0.7%).

In addition, in two of 257 (0.8%) samples with available genomic copy number profiles, an *ALK* gene amplification was detected. One of these samples (NB1418T) also showed a R1275Q mutation (mutated allele fraction 73%; Table 2).

All *ALK* mutated samples were also tested by Sanger sequencing which confirmed all *ALK* mutations occurring at a clonal level with a mutated allele fraction >20%. Because of the limits of

Published OnlineFirst June 9, 2015; DOI: 10.1158/1078-0432.CCR-15-0423

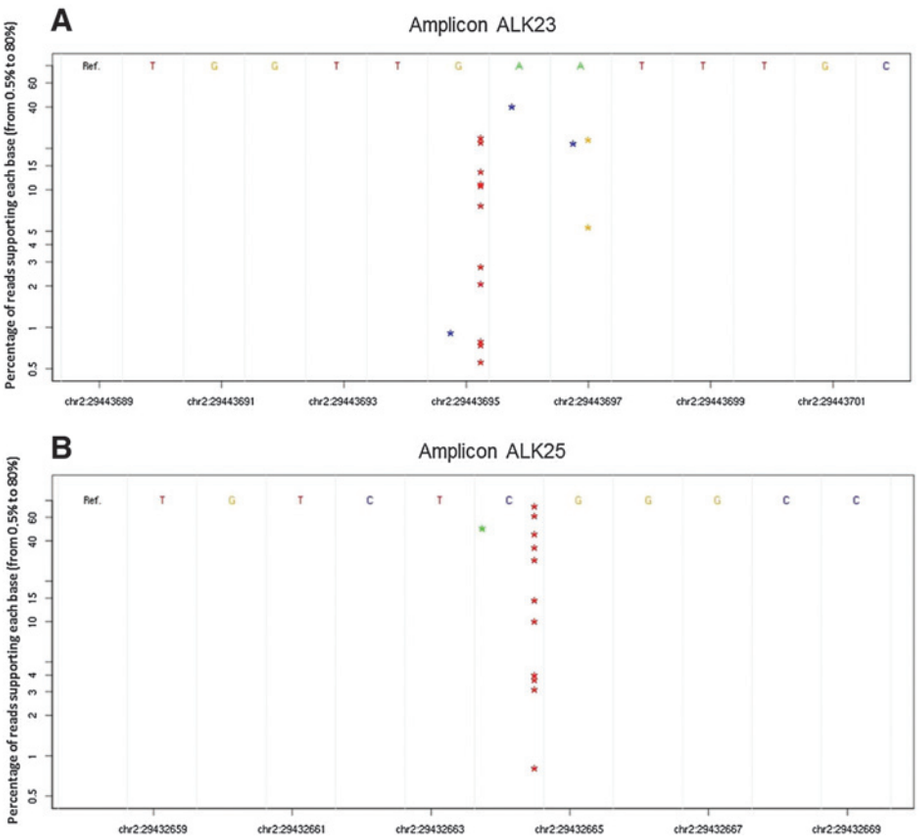

Figure 2.
Mutated allele fractions (frequency distribution of mutated *ALK* allele) at the *ALK* F1174 and R1275 hotspots detected in 27 samples. The *x*-axis represents the genomic coordinates of the targeted region, the *y*-axis represents the percentage of high quality reads supporting each base (logarithmic scale). Bases A, C, G, and T are represented with green, blue, yellow, and red colors, respectively, and the base corresponding to the reference genome sequence is reported above the graph, for the forward strand. A, chr2:29443689–29443702 region encompassing the exon 23 hotspot F1174 (positions 29443695–29443697) ±5 bases. Eleven mutations are detected at the position 29443695 (G>T), one detected at the position 29443696 (A>C) and three detected at the position 29443697 (A>C/G). B, chr2:29432658–29432669 region encompassing the exon 25 hotspot R1275 (position 29432664) ± 5 bases. Twelve mutations are detected at the position 29432664 (C>T/A).

detection and due to the background noise generally present in the Sanger elecropherograms, *ALK* mutations would not have been retained by Sanger sequencing in subclonal cases.

Correlation of *ALK* aberrations (mutations and/or amplification) with clinical parameters in neuroblastoma

A correlation between the presence of an *ALK* aberration (mutations and/or amplification) and *MYCN* amplification was observed (Table 3, panel A), with an enrichment of F1174 *ALK* mutations in tumors harboring MYCN amplification ($P < 0.0001$). There were no other statistically significant correlations with clinical parameters (Table 3, panel A).

Furthermore, no statistically significant correlations between the *ALK* status and main clinical parameters were observed among patients whose tumors harbored *ALK* mutations either at a clonal or subclonal level, respectively.

FISH analysis of MYCN status correlated with the tumor cell content determined by H&E staining, and in no instance was heterogeneous MYCN amplification observed. In particular, in cases with *ALK* mutations detected at a subclonal level, MYCN status determined by FISH was homogeneous throughout all tumor cells, and in amplified cases concerned all tumor cells (>50% of cells in the sample).

Impact of *ALK* mutations on survival

The overall survival of patients with *ALK* wild-type versus *ALK*-mutated and/or *ALK*-amplified tumors was compared, and Kaplan–Meier analysis showed a statistically significant poorer OS in patients whose tumors harbored an *ALK* aberration ($P < 0.02$; Fig. 3A). However, no statistically significant differences were found in PFS between these two patient groups. A statistically significant difference in OS was observed between patients with *ALK* F1174-mutated tumors versus all other patients ($P = 0.0014$; Fig. 3B). The comparison of survival of patients with *ALK* wild-type or *ALK* aberrations, with or without MYCN amplification showed a poorer OS in patients whose tumors harbor MYCN amplification, with or without *ALK* aberration (Fig. 3C).

Multivariate analysis of OS using a Cox's regression model further confirmed that in this series, independent predictors of poor outcome are INSS stage IV disease and MYCN amplification, and that *ALK* mutational status does not add prognostic information to the clinical parameters "INSS stage" and "MYCN status" (Table 3, panel B). No statistically significant differences of OS and PFS in patients with *ALK* mutations at a clonal versus subclonal level were observed (log-rank test: $P = 0.2$ and $P = 0.98$, respectively).

Discussion

In order to determine the frequency of *ALK* mutations in diagnostic neuroblastoma samples with a higher sensitivity than conventional sequencing methods, we have used ultra-deep sequencing to analyze a large series of representative neuroblastoma samples (Supplementary Table S1).

Published OnlineFirst June 9, 2015; DOI: 10.1158/1078-0432.CCR-15-0423

Table 2. Clinical and tumor genetic data of patients harboring *ALK* mutations

Sample	Age at diagnosis (mo)	INSS stage	Relapse (yes or no)	Follow-up (mo)	Status	Interval diagnosis-relapse (mo)	Tumoral cells (%)	chr 2p copy number at *ALK* locus	MYCN status	*ALK* amplification status	*ALK* F1174 status as detected by Hiseq (% of mutated allele)	*ALK* R1275 status as detected by Hiseq (% of mutated allele)
NB0211T	20	Loc	No	155	Alive	NA	90	3	MN-NA	ALK-NA	/	28.647
NB0824T	3	4	Yes	13	DOD	3	95	3	MN-NA	ALK-NA	22.957	/
NB0366T	3	Loc	No	98	Alive	NA	80	3	MN-NA	ALK-NA	20.899	/
NB0183T	35	4	No	109	Alive	NA	90	3	MNA	ALK-NA	0.787	/
NB0194T	40	4	Yes	10	DOD	7	>50	2–3	MNA	ALK-NA	4.914	/
NB0085T	2	4s	No	61	Alive	NA	100	3	MN-NA	ALK-NA	/	61.722
NB0222T	3	Loc	No	63	Alive	NA	>50	2	MN-NA	ALK-NA	/	49.206
NB0230T	43	4	Yes	21	DOD	11	>50	2	MNA	ALK-NA	0.562	/
NB0789T	33	Loc	No	56	Alive	NA	80	3	MN-NA	ALK-NA	22.854	/
NB0233T	34	4	No	49	Alive	NA	>50	4	MNA	ALK-NA	/	3.648
NB0012T	13	4	Yes	7	DOD	5	90	2	MNA	ALK-NA	7.657	/
NB0372T	10	Loc	No	24	Alive	NA	90	3	MN-NA	ALK-NA	/	61.443
NB1244T	13	4	No	40	DOD	NA	90	2	MNA	ALK-NA	13.46	/
NB0308T	3	Loc	Yes	92	Alive	21	>50	3	MN-NA	ALK-NA	/	14.419
NB0186T	10	4	No	6	DOD	NA	80	2	MNA	ALK-NA	10.534	/
NB0231T	50	4	Yes	27	DOD	19	90	4	MNA	ALK-NA	2.750	/
NB1129T	31	4	No	33	Alive	NA	95	2	MNA	ALK-NA	/	3.994
NB0535T	4	Loc	Yes	210	Alive	5	80	2–3	MN-NA	ALK-NA	21.198	/
NB0014T	4	4	Yes	10	DOD	10	90	3	MNA	ALK-NA	0.744	/
NB0540T	10	4	No	235	Alive	NA	70	3–4	MN-NA	ALK-NA	/	0.811
NB1057T	35	4	No	39	Alive	NA	50	2	MNA	ALK-NA	/	3.109
NB0284T	44	Loc	Yes	6	DOD	6	90	3	MNA	ALK-NA	0.917	/
NB0920T	4	4	Yes	51	Alive	14	90	2	MN-NA	ALK-NA	38.955	/
NB0984T	24	4	Yes	14	DOD	11	>50	2	MNA	ALK-NA	/	45.123
NB1001T	12	Loc	No	5	Alive	NA	90	3	MN-NA	ALK-NA	/	35.499
NB1418T	15	4	Yes	6	DOD	6	95	3	MNA	ALK-A	/	73.001
NB1253T	17	4	No	140	Alive	NA	>60	2	MNA	ALK-NA	5.323	/

NOTE: For 27 patients, *ALK* mutations were detected at diagnosis by deep sequencing.

Abbreviations: ALK-A, ALK amplified; ALK-NA, ALK not-amplified; D, diagnosis; DOD, dead of disease; INSS, International Neuroblastoma Staging System; Loc, local tumor (stages 1, 2a, 2b or 3); MNA, MYCN amplification; MN-NA, MYCN non-amplified; NA, Not-applicable; /: not applicable.

Published OnlineFirst June 9, 2015; DOI: 10.1158/1078-0432.CCR-15-0423

Table 3. Correlation between *ALK* status and main clinical factors in neuroblastoma (A) and multivariate analysis (B; $N = 276$)

A

	ALK status							
		Alteration of *ALK*						$\chi 2$ Test
Age at the diagnosis	***ALK* WT**	**All *ALK* alterations**	**Clonal**	**Subclonal**	**F1174 mut**	**R1275 mut**	**Amplification**	***P* value**
<18 months	141	17	9	7	9	7[a]	2[a]	NS
≥18 months	107	11	3	8	6	5	0	
INSS stage								
4	107	18	4	13	11	6[a]	2[a]	NS
Loc or 4s	138	10	8	2	4	6	0	
MD	3	0	0	0	0	0	0	
MYCN status								
MYCN amp	39	16	2	13	10	5[a]	2[a]	$P < 0.0001$
MYCN non-ampl	209	12	10	2	5	7	0	

B

	Multivariate analysis	
Variables	**HR (95% CI)**	***P***
INSS stage (unfavorable vs. favorable)	7.62 (3.82–15.16)	<0.0001
MYCN (amplified vs. nonamplified)	3.85 (2.38–6.21)	<0.0001
age at diagnosis (>18 mo vs. <18 mo)	NS	NS
ALK (mutated vs. nonmutated)	NS	NS

[a]Both *ALK* amplification and R1275 mutation detected in one tumor.

Abbreviations: CI, confidence interval; clonal, allele frequency >20%; INSS, International Neuroblastoma Staging System; MD, missing data; NS, not significant; subclonal, allele frequency <20%.

Traditional Sanger sequencing has been widely used in clinical laboratories for mutation testing, but the sensitivity is limited to the detection of 20% to 30% of mutated alleles in a wild-type background (25). A higher sensitivity has been shown for droplet digital PCR (ddPCR) and NGS techniques (25, 27). Indeed, a limit of detection of 2% of mutated allele fractions has been evidenced for *BRAF* mutations using NGS methods (29). We have reported on a sensitivity limit of 0.17% using PGM technology for detection of *ALK* mutations in a series of diagnostic and relapse neuroblastoma samples (30).

Different algorithms, such as ABSOLUTE, have been described to detect mutations with low mutated allele fractions (31). However, these algorithms have not been developed specifically for ultra-deep sequencing data. Thus, in this study, a custom approach has been used to define mutations with very low mutated allele fractions in deep-sequencing data.

In this study, the targeted sequencing method achieved a very high depth of coverage over the region of interest (mean coverage 33,000X). On the basis of this coverage, a mutated allele fraction of 0.21% or more was considered significantly different from the germline controls, which is well below the lower limit defined in the technical specifications of Hiseq Illumina. This calculated sensitivity is considered relevant only if (i) analyzed data correspond to similar depth of coverage, (ii) sequencing is performed with the same technology, (iii) controls show similar low variability, and (iv) the targeted region has a base environment similar to the regions analyzed in this experiment. This detection limit also corresponds to the theoretical limit of detection based on the DNA input for one experiment (50 ng of DNA, equivalent to approximately 5,000 diploid genomes).

Between the different mutation types, a higher mean mutated allele fraction was observed in the R1275 cases (mean of mutated allele fractions: 11.6 vs. 29.5 in F1174 vs. R1275 cases, respectively; $P = 0.02$, t test). When considering chr2p status, in cases with three copies of chr2, the mutated allele most likely concerns the non-duplicated chr2p for F1174, and the duplicated chr2p for R1275 (Table 2). This might further support the hypothesis that R1275 mutations are less aggressive than F1174 mutations, and that more copies of the R1275 mutated allele are necessary to transfer selective advantage to the tumor cells, as previously suggested (32, 33).

Previous studies describing *ALK* mutations in neuroblastoma samples, frequently analyzing the whole tyrosine kinase domain, have used conventional sequencing methods, such as Sanger sequencing, or whole-genome/whole-exome sequencing with standard resolution. The incidence of *ALK* mutations observed in these studies varies from 6% to 12% of all neuroblastoma cases (15, 16, 18–21). In our cohort, studying only exons 23 and 25 of the *ALK* gene, 27 of 276 neuroblastoma (9.8%) presented an *ALK* mutation. An incidence of only 4.3% would have been observed by Sanger sequencing, with the incidence doubling when moving to ultra-sensitive deep sequencing.

To date, in neuroblastoma, the co-occurrence of an *ALK* hotspot mutation and amplification has been reported only for a cell line: CLB-GE harbors both the F1174V mutation and an *ALK* high level amplification (15). In this series, one sample had both *ALK* amplification and a R1275 mutation, indicating that, although rare, these alterations are not mutually exclusive (Table 2). A mutated allele fraction of 73% in the context of a genomic amplification of >10 copies suggested that the *ALK* gene underwent amplification before an R1275 mutational event with subsequent further amplification rounds.

ALK F1174L mutations have been reported in a higher frequency in *MYCN*-amplified tumors (19). The co-occurrence of *ALK* F1174L and *MYCN* amplification probably represents a cooperative effect between both alterations in neuroblastoma, which might explain the particularly poor survival of these patients (33, 34).

In vitro and *in vivo* studies have indicated the efficacy of ALK inhibitors on cells harboring *ALK* mutations at a clonal level (21, 28). It now remains to be determined whether tumor populations composed of subclones harboring *ALK* R1275 or F1174 mutations have different growth properties and different responses to ALK inhibitors in *in vitro* and *in vivo* experimental systems.

Published OnlineFirst June 9, 2015; DOI: 10.1158/1078-0432.CCR-15-0423

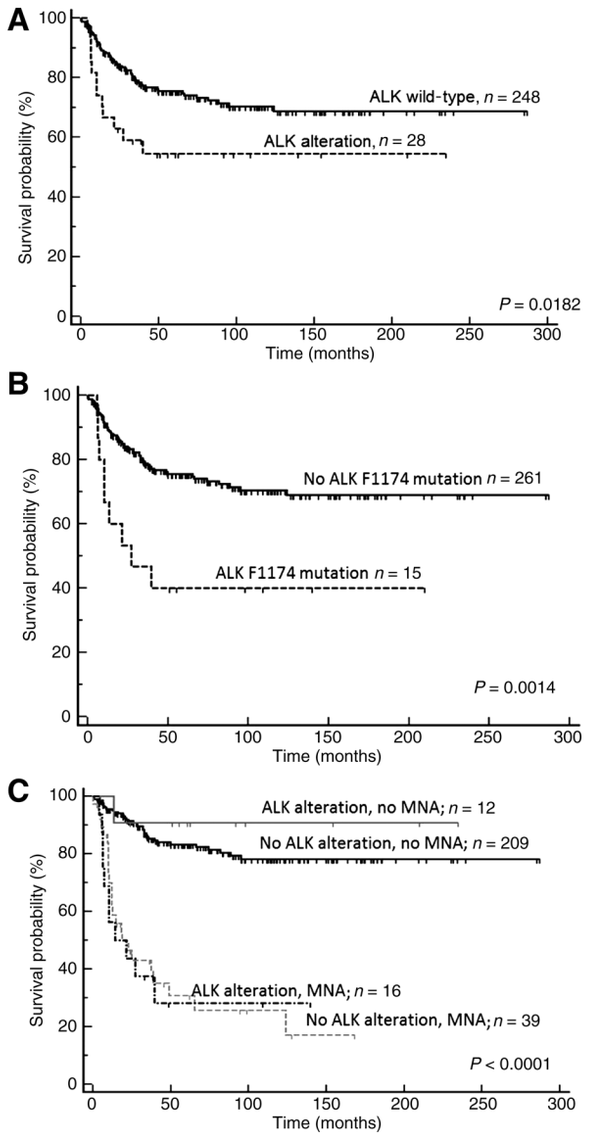

Figure 3.
OS analysis. A, OS according to the presence or absence of somatic *ALK* aberrations. Neuroblastoma patients whose tumors harbor an *ALK* alteration (*ALK* mutations and/or amplification) show a decreased overall survival (5-year OS 54% ±9.8% versus 75% ±2.9%; log-rank test, $P = 0.0182$). B, OS according to the presence or absence of the F1174 mutation. Neuroblastoma patients whose tumor show a F1174 mutation show a poorer OS (5-year OS 40% ±12.6% versus 75% ±2.8%; log-rank test, $P = 0.0014$). C, OS according to MYCN and *ALK* status (MYCN amplification vs. no amplification; *ALK* alteration versus no alteration). Kaplan–Meier analysis indicates that the poorer OS observed in patients with tumors showing an *ALK* alteration is dependent on MYCN amplification (5-year OS 90% ±8.6%, 83% ±2.8%, 30% ±8.5%, 28% ±12.2%, respectively; log-rank test, $P < 0.0001$).

The observation of *ALK*-mutated subclones at diagnosis suggests the coexistence of *ALK* nonmutated and *ALK*-mutated cells, which might coexist in an advantageous equilibrium and might crucially affect the dynamics of cancer progression at a later stage. Cooperation of different tumor cell subsets has been reported to contribute to the malignant cancer phenotype (30, 32). Single cell experiments and *in situ* approaches will enable to elucidate how *ALK*-mutated cells are distributed throughout a neuroblastoma tumor and how these cells might potentially collaborate with cells with different genetic alterations.

A higher frequency of *ALK* mutations at relapse of neuroblastoma has recently been reported, with the possibility of expansion of a minor *ALK*-mutated subclone at diagnosis to a dominant *ALK*-mutated clone at relapse (26). Further detailed sequencing studies in larger series of diagnosis-relapse samples will be required to elucidate the role of subclonal *ALK* mutations in clonal evolution and progression of neuroblastoma.

In conclusion, given the oncogenic role of *ALK*, the possibility of evolution of *ALK* mutated clones from diagnosis to relapse and the possibility to target *ALK* mutations with ALK inhibitors such as crizotinib (PF-02341066) or other second-generation ALK inhibitors such as LDK378 (Novartis Pharmaceuticals), the determination of the exact genetic *ALK* status in all neuroblastoma is crucial (21, 29). We clearly demonstrate the advantages of deep-sequencing NGS technology for the detection of mutational events in a common pediatric cancer. Our approach, relative to conventional methods, has shown several advantages, including (i) *in vitro* library construction of a large number of samples, (ii) high resolution, (iii) short time analysis, and (iv) high accuracy. Owing to the higher sensitivity of deep sequencing, it is very likely that, in the near future and with growing experience, these techniques will replace conventional methods for mutation detection.

The high-resolution technique identifies clonal and subclonal mutational events, thus doubling the number of identified *ALK* mutation events compared with those detected with conventional sequencing techniques. To date, no formal recommendation for targeted therapy in a context of low subclonal events can be given. Indeed, in other pathologies, targeted therapies such as dabrafenib for V600E/K mutations in melanoma are most frequently proposed in a context of mutation detection using standard resolution techniques which do not reveal lower mutated allele fractions below 5% to 10% (35). Our findings now highlight the importance of further functional studies analyzing the interactions between *ALK*-mutated and nonmutated subclones on the one hand, and the possibilities of clonal evolution on the other hand. Such studies should especially focus on the analysis of readily accessible surrogate samples, such as serial blood samples for the study of ctDNA.

Disclosure of Potential Conflicts of Interest

No potential conflicts of interest were disclosed.

Authors' Contributions

Conception and design: D. Valteau-Couanet, O. Delattre, G. Schleiermacher
Development of methodology: A. Bellini, Q. Leroy, T. Rio Frio, G. Schleiermacher
Acquisition of data (provided animals, acquired and managed patients, provided facilities, etc.): Q. Leroy, G. Pierron, V. Combaret, E. Lapouble, H. Rubie, E. Thebaud, C. Bergeron, N. Buchbinder, S. Taque, A. Auvrignon, J. Michon, I. Janoueix-Lerosey, G. Schleiermacher
Analysis and interpretation of data (e.g., statistical analysis, biostatistics, computational analysis): A. Bellini, V. Bernard, C. Bergeron, I. Janoueix-Lerosey, G. Schleiermacher
Writing, review, and/or revision of the manuscript: A. Bellini, V. Bernard, G. Pierron, V. Combaret, P. Chastagner, A.S. Defachelles, C. Bergeron, D. Valteau-Couanet, O. Delattre, G. Schleiermacher
Administrative, technical, or material support (i.e., reporting or organizing data, constructing databases): A. Bellini, G. Pierron, E. Lapouble, N. Clement, O. Delattre, G. Schleiermacher
Study supervision: G. Schleiermacher

Acknowledgments

The authors thank the following colleagues for their contribution to this study: Catherine Devoldere, Paul Fréneaux, Vannina Giacobbi-Milet, Hayet Hanbli, Philippe Le Moine, Odile Minckes, Isabelle Pellier, Michel Peuchmaur, Dominique Plantaz, Emmanuel Plouvier, and Nicolas Sirvent.

Grant Support

This work was supported by the Annenberg foundation and the Ligue Nationale Contre le Cancer (équipe labellisée). Funding was also obtained from SiRIC/INCa (Grant INCa-DGOS-4654) and from the CEST of Institute Curie and by the Associations Enfants et Santé, Association Hubert Gouin Enfance et Cancer, Les Bagouz à Manon, Les amis de Claire. Next generation experiments (NGS) were conducted on the Institute Curie's ICGex NGS platform funded by the EQUIPEX "investissements d'avenir" program (ANR-10-EQPX-03) and ANR10-IneuroblastomaS-09-08 from the Agence Nationale de le Recherche, and by the Canceropôle Ile de-France.

The costs of publication of this article were defrayed in part by the payment of page charges. This article must therefore be hereby marked *advertisement* in accordance with 18 U.S.C. Section 1734 solely to indicate this fact.

Received February 20, 2015; revised May 4, 2015; accepted May 25, 2015; published OnlineFirst June 9, 2015.

References

1. Gerlinger M, Rowan AJ, Horswell S, Larkin J, Endesfelder D, Gronroos E, et al. Intratumor heterogeneity and branched evolution revealed by multiregion sequencing. N Engl J Med 2012;366:883–92.
2. Swanton C. Intratumor heterogeneity: evolution through space and time. Cancer Res 2012;72:4875–82.
3. Anderson K, Lutz C, van Delft FW, Bateman CM, Guo Y, Colman SM, et al. Genetic variegation of clonal architecture and propagating cells in leukaemia. Nature 2011;469:356–61.
4. Burrell RA, McGranahan N, Bartek J, Swanton C. The causes and consequences of genetic heterogeneity in cancer evolution. Nature 2013;501:338–45.
5. Crockford A, Jamal-Hanjani M, Hicks J, Swanton C. Implications of intratumour heterogeneity for treatment stratification. J Pathol 2014;232:264–73.
6. Greaves M, Maley CC. Clonal evolution in cancer. Nature 2012;481:306–13.
7. Newburger DE, Kashef-Haghighi D, Weng Z, Salari R, Sweeney RT, Brunner AL, et al. Genome evolution during progression to breast cancer. Genome Res 2013;23:1097–108.
8. Eirew P, Steif A, Khattra J, Ha G, Yap D, Farahani H, et al. Dynamics of genomic clones in breast cancer patient xenografts at single-cell resolution. Nature 2015;518:422–6.
9. Landau DA, Carter SL, Stojanov P, McKenna A, Stevenson K, Lawrence MS, et al. Evolution and impact of subclonal mutations in chronic lymphocytic leukemia. Cell 2013;152:714–26.
10. Janoueix-Lerosey I, Schleiermacher G, Michels E, Mosseri V, Ribeiro A, Lequin D, et al. Overall genomic pattern is a predictor of outcome in neuroblastoma. J Clin Oncol 2009;27:1026–33.
11. Molenaar JJ, Koster J, Zwijnenburg DA, van Sluis P, Valentijn LJ, van der Ploeg I, et al. Sequencing of neuroblastoma identifies chromothripsis and defects in neuritogenesis genes. Nature 2012;483:589–93.
12. Pugh TJ, Morozova O, Attiyeh EF, Asgharzadeh S, Wei JS, Auclair D, et al. The genetic landscape of high-risk neuroblastoma. Nat Genet 2013;45:279–84.
13. Sausen M, Leary RJ, Jones S, Wu J, Reynolds CP, Liu X, et al. Integrated genomic analyses identify ARID1A and ARID1B alterations in the childhood cancer neuroblastoma. Nat Genet 2013;45:12–7.
14. Schleiermacher G, Janoueix-Lerosey I, Ribeiro A, Klijanienko J, Couturier J, Pierron G, et al. Accumulation of segmental alterations determines progression in neuroblastoma. J Clin Oncol 2010;28:3122–30.
15. Janoueix-Lerosey I, Lequin D, Brugières L, Ribeiro A, de Pontual L, Combaret V, et al. Somatic and germline activating mutations of the ALK kinase receptor in neuroblastoma. Nature 2008;455:967–70.
16. Mossé YP, Laudenslager M, Longo L, Cole KA, Wood A, Attiyeh EF, et al. Identification of ALK as a major familial neuroblastoma predisposition gene. Nature 2008;455:930–5.
17. Schleiermacher G, Janoueix-Lerosey I, Delattre O. Recent insights into the biology of neuroblastoma. Int J Cancer 2014;135:2249–61.
18. Chen Y, Takita J, Choi YL, Kato M, Ohira M, Sanada M, et al. Oncogenic mutations of ALK kinase in neuroblastoma. Nature 2008;455:971–4.
19. De Brouwer S, De Preter K, Kumps C, Zabrocki P, Porcu M, Westerhout EM, et al. Meta-analysis of neuroblastomas reveals a skewed ALK mutation spectrum in tumors with MYCN amplification. Clin Cancer Res 2010;16:4353–62.
20. Carén H, Abel F, Kogner P, Martinsson T. High incidence of DNA mutations and gene amplifications of the ALK gene in advanced sporadic neuroblastoma tumours. Biochem J 2008;416:153–9.
21. Bresler SC, Weiser DA, Huwe PJ, Park JH, Krytska K, Ryles H, et al. ALK mutations confer differential oncogenic activation and sensitivity to ALK inhibition therapy in neuroblastoma. Cancer Cell 2014;26:682–94.
22. Cazes A, Louis-Brennetot C, Mazot P, Dingli F, Lombard B, Boeva V, et al. Characterization of rearrangements involving the ALK gene reveals a novel truncated form associated with tumor aggressiveness in neuroblastoma. Cancer Res 2013;73:195–204.
23. Li H, Durbin R. Fast and accurate short read alignment with Burrows-Wheeler transform. Bioinformatics 2009;25:1754–60.
24. McKenna A, Hanna M, Banks E, Sivachenko A, Cibulskis K, Kernytsky A, et al. The Genome Analysis Toolkit: a MapReduce framework for analyzing next-generation DNA sequencing data. Genome Res 2010;20:1297–303.
25. Ihle MA, Fassunke J, König K, Grünewald I, Schlaak M, Kreuzberg N, et al. Comparison of high resolution melting analysis, pyrosequencing, next generation sequencing and immunohistochemistry to conventional Sanger sequencing for the detection of p.V600E and non-p.V600E BRAF mutations. BMC Cancer 2014;14:13.
26. Schleiermacher G, Javanmardi N, Bernard V, Leroy Q, Cappo J, Rio Frio T, et al. Emergence of new ALK mutations at relapse of neuroblastoma. J Clin Oncol 2014;32:2727–34.
27. Combaret V, Iacono I, Bellini A, Bréjon S, Bernard V, Marabelle A, et al. Detection of tumor ALK status in neuroblastoma patients using peripheral blood. Cancer Med 2015;4:540–50.
28. Bresler SC, Wood AC, Haglund EA, Courtright J, Belcastro LT, Plegaria JS, et al. Differential inhibitor sensitivity of anaplastic lymphoma kinase variants found in neuroblastoma. Sci Transl Med 2011;3:108ra114.
29. Barone G, Anderson J, Pearson ADJ, Petrie K, Chesler L. New strategies in neuroblastoma: therapeutic targeting of MYCN and ALK. Clin Cancer Res 2013;19:5814–21.
30. Axelrod R, Axelrod DE, Pienta KJ. Evolution of cooperation among tumor cells. Proc Natl Acad Sci U S A 2006;103:13474–9.
31. Carter SL, Cibulskis K, Helman E, McKenna A, Shen H, Zack T, et al. Absolute quantification of somatic DNA alterations in human cancer. Nat Biotechnol 2012;30:413–21.
32. Cleary AS, Leonard TL, Gestl SA, Gunther EJ. Tumour cell heterogeneity maintained by cooperating subclones in Wnt-driven mammary cancers. Nature 2014;508:113–7.
33. Berry T, Luther W, Bhatnagar N, Jamin Y, Poon E, Sanda T, et al. The ALK (F1174L) mutation potentiates the oncogenic activity of MYCN in neuroblastoma. Cancer Cell 2012;22:117–30.
34. Zhu S, Lee J-S, Guo F, Shin J, Perez-Atayde AR, Kutok JL, et al. Activated ALK collaborates with MYCN in neuroblastoma pathogenesis. Cancer Cell 2012;21:362–73.
35. Robert C, Karaszewska B, Schachter J, Rutkowski P, Mackiewicz A, Stroiakovski D, et al. Improved overall survival in melanoma with combined dabrafenib and trametinib. N Engl J Med 2015;372:30–9.

Published OnlineFirst June 9, 2015; DOI: 10.1158/1078-0432.CCR-15-0423

Clinical Cancer Research

Deep Sequencing Reveals Occurrence of Subclonal *ALK* Mutations in Neuroblastoma at Diagnosis

Angela Bellini, Virginie Bernard, Quentin Leroy, et al.

Clin Cancer Res 2015;21:4913-4921. Published OnlineFirst June 9, 2015.